J|A|C|S
ARTICLES
Published on Web 06/18/2003

Electrochemically Switchable Hydrogen-Bonded Molecular Shuttles

Alessio Altieri,[‡] Francesco G. Gatti,[†] Euan R. Kay,[†] David A. Leigh,*[,†] David Martel,[‡] Francesco Paolucci,*[,‡] Alexandra M. Z. Slawin,[§] and Jenny K. Y. Wong[†]

Contribution from the School of Chemistry, University of Edinburgh, The King's Buildings, West Mains Road, Edinburgh EH9 3JJ, United Kingdom, Dipartimento di Chimica "G. Ciamician", Università degli Studi di Bologna, v. F. Selmi 2, 40126, Bologna, Italy, and Department of Chemistry, University of St. Andrews, St. Andrews KY16 9ST, United Kingdom

Received March 20, 2003; E-mail: david.leigh@ed.ac.uk; paolucci@ciam.unibo.it

Abstract: A series of [2]rotaxanes containing succinamide and naphthalimide hydrogen-bonding stations for a benzylic amide macrocycle is described. Electrochemical reduction and oxidation of the naphthalimide group alters its ability to form hydrogen bonds to the macrocycle to such a degree that redox processes can be used to switch the relative macrocycle-binding affinities of the two stations in a rotaxane by over 8 orders of magnitude. The structure of the neutral [2]rotaxane in solution is established by ^{1}H NMR spectroscopy and shows that the macrocycle exhibits remarkable positional integrity for the succinamide station in a variety of solvents. Cyclic voltammetry experiments allow the simultaneous stimulation and observation of a redox-induced dynamic process in the rotaxane which is both reversible and cyclable. Model compounds in which various conformational and co-conformational changes are prohibited demonstrate unequivocally that the redox response is the result of shuttling of the macrocycle between the two stations. At room temperature in tetrahydrofuran the electrochemically induced movement of the macrocycle between the two stations takes ~50 μs.

Introduction

Natural[1] and artificial[2] devices that function through mechanical motion at the molecular level require a nanoscale structure that restricts the freedom of movement of the various components coupled with a process—usually chemical—to power and control their motions. For the design of prototypical synthetic systems, chemists have taken inspiration from the structural elements of machinery from the macroscopic world.[3] Taking this analogy too far in terms of process must be cautioned, however, since the modes of action for useful movement at the molecular and macroscopic levels are very different. In the macroscopic world, objects do not move until provided with specific energy to do so. In a mechanical machine, this is often through a directional stimulus (i.e., when work is done to move components in a particular way). At the molecular level, molecules—and their parts—are constantly moving above 0 K and it is the directional control of this motion which Nature uses to perform useful mechanical tasks.[1]

'Molecular shuttles' provide a promising basis for artificial molecular machines. Various types of rotaxane[4] structures permit large amplitude, largely independent, motions of the mechanically interlocked components, and the noncovalent bond-directed routes to their synthesis offer a process for controlling the relative positioning of the components through the interactions that 'live on' in the final products.[5] In a rotaxane with two different binding sites ('stations') in the thread, the macrocycle distributes itself between the stations according to the difference in the macrocycle-binding energies and the temperature. If a suitably large difference in macrocycle affinity between the two stations exists, the macrocycle resides overwhelmingly in one

[†] University of Edinburgh.
[‡] Università degli Studi di Bologna.
[§] University of St. Andrews.

(1) *Molecular Motors*; Schliwa, M., Ed.; Wiley-VCH: Weinheim, 2003.
(2) With the notable exception of liquid crystals, the first artificial devices that rely on mechanical motion at the molecular level for a practical function are the catenanes and rotaxanes used to configure the remarkable solid-state switches and logic gates developed by Stoddart and Heath. (a) Collier, C. P.; Wong, E. W.; Bělohradský, M.; Raymo, F. M.; Stoddart, J. F.; Kuekes, P. J.; Williams, R. S.; Heath, J. R. *Science* **1999**, *285*, 391−394. (b) Wong, E. W.; Collier, C. P.; Bělohradský, M.; Raymo, F. M.; Stoddart, J. F.; Heath, J. R. *J. Am. Chem. Soc.* **2000**, *122*, 5831−5840. (c) Collier, C. P.; Jeppesen, J. O.; Luo, Y.; Perkins, J.; Wong, E. W.; Heath, J. R.; Stoddart, J. F. *J. Am. Chem. Soc.* **2001**, *123*, 12632−12641. (d) Luo, Y.; Collier, C. P.; Jeppesen, J. O.; Nielsen, K. A.; Delonno, E.; Ho, G.; Perkins, J.; Tseng, H.-R.; Yamamoto, T.; Stoddart, J. F.; Heath, J. R. *Chem. Phys. Chem.* **2002**, *3*, 519−525.
(3) See, for example, analogic molecular versions of gears: (a) Iwamura, H.; Mislow, K. *Acc. Chem. Res.* **1988**, *21*, 175−182. Turnstiles: (b) Bedard, T. C.; Moore, J. S. *J. Am. Chem. Soc.* **1995**, *117*, 10662−10671. Brakes: (c) Kelly, T. R.; Bowyer, M. C.; Bhaskar, K. V.; Bebbington, D.; Garcia, A.; Lang, F.; Kim, M. H.; Jette, M. P. *J. Am. Chem. Soc.* **1994**, *116*, 3657−3658. Ratchets: (d) Kelly, T. R.; Tellitu, I.; Sestelo, J. P. *Angew. Chem., Int. Ed. Engl.* **1997**, *36*, 1866−1868. (e) Kelly, T. R.; Sestelo, J. P.; Tellitu, I. *J. Org. Chem.* **1998**, *63*, 3655−3665. Rotors: (f) Schoevaars, A. M.; Kruizinga, W.; Zijlstra, R. W. J.; Veldman, N.; Spek, A. L.; Feringa, B. L. *J. Org. Chem.* **1997**, *62*, 4943−4948. Unidirectional spinning motors: (g) Kelly, T. R.; De Silva, H.; Silva, R. A. *Nature* **1999**, *401*, 150−152. (h) Koumura, N.; Zijlstra, R. W. J.; van Delden, R. A.; Harada, N.; Feringa, B. L. *Nature* **1999**, *401*, 152−155. (i) Kelly, T. R.; Silva, R. A.; De Silva, H.; Jasmin, S.; Zhao, Y. *J. Am. Chem. Soc.* **2000**, *122*, 6935−6949. (j) Koumura, N. L.; Geertsema, E. M.; van Gelder, M. B.; Meetsma, A.; Feringa, B. L. *J. Am. Chem. Soc.* **2002**, *124*, 5037−5051.
(4) *Molecular Catenanes, Rotaxanes and Knots*; Sauvage, J.-P., Dietrich-Buchecker, C., Eds.; Wiley-VCH: Weinheim, 1999.

10.1021/ja0352552 CCC: $25.00

positional isomer or co-conformation.[6] In stimuli-responsive molecular shuttles,[7−11] an external trigger is used to chemically modify the system and alter the noncovalent intercomponent interactions such that the second macrocycle-binding site becomes energetically more favored causing translocation of the macrocycle along the thread to the second station (Figure 1). The system can be returned to its original state by using a second chemical transformation to restore the initial order of station binding affinities. Performed consecutively, these two steps allow the 'machine' to carry out a complete cycle of shuttling motion. The movement of the macrocycle from station to station is thus caused by using chemical reactions to put the molecule into nonequilibrium co-conformations and then allowing the background thermal energy to drive the macrocycle to the new global minimum (i.e., through biased Brownian motion).

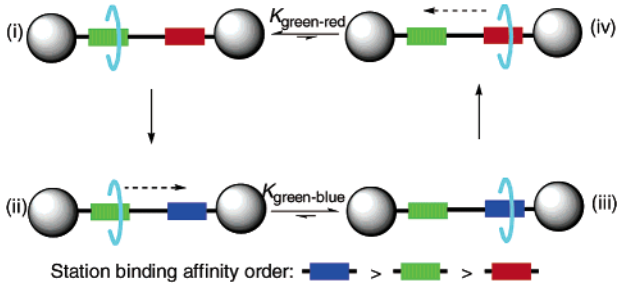

Figure 1. Translational submolecular motion in a stimuli-responsive molecular shuttle: (i) the macrocycle initially resides on the preferred (green) station; (ii) a reaction occurs (red → blue) changing the relative binding potentials of the two stations such that (iii) the macrocycle 'shuttles' to the now-preferred (blue) station. If the reverse reaction (blue → red) now occurs, (iv) the components return to their original positions. The energy available to do mechanical work through shuttling in such a cycle is the sum of the difference in macrocycle binding energies of the two stations in each of the two states (i.e., $\Delta\Delta G_{green-red} + \Delta\Delta G_{blue-green}$).

We recently reported the real-time observation of macrocycle translocation in such a stimuli-responsive molecular shuttle following the photochemically induced reduction of the naphthalimide unit in rotaxane **1**.[8f] In fact, we originally designed **1** as an electrochemically switchable system.[12] Electrochemistry is potentially an attractive method through which to modulate the behavior of molecular devices because it can be easily and rapidly turned on and off while also offering a reagent and waste-free procedure. Obviously, an important attribute of any 'molecular machine' is that for the submolecular motion to be useful it must be detectable through some change in the system's

(5) For reviews on the development of interlocked molecules as molecular machines, see: (a) Balzani, V.; Gómez-López, M.; Stoddart, J. F. *Acc. Chem. Res.* **1998**, *31*, 405−414. (b) Sauvage, J.-P. *Acc. Chem. Res.* **1998**, *31*, 611−619. (c) Chambron, J.-C.; Sauvage, J.-P. *Chem. Eur. J.* **1998**, *4*, 1362−1366. (d) Balzani, V.; Credi, A.; Raymo, F. M.; Stoddart, J. F. *Angew. Chem., Int. Ed.* **2000**, *39*, 3348−3391. (e) Asfari, Z.; Vicens, J. *J. Inclusion Phenom. Macro. Chem.* **2000**, *36*, 103−118. (f) Pease, A. R.; Jeppesen, J. O.; Stoddart, J. F.; Luo, Y.; Collier, C. P.; Heath, J. R. *Acc. Chem. Res.* **2001**, *34*, 433−444. (g) Ballardini, R.; Balzani, V.; Credi, A.; Gandolfi, M. T.; Venturi, M. *Acc. Chem. Res.* **2001**, *34*, 445−455. (h) Collin, J.-P.; Dietrich-Buchecker, C.; Gaviña, P.; Jimenez-Molero, M. C.; Sauvage, J.-P. *Acc. Chem. Res.* **2001**, *34*, 477−487. (i) *Molecular Machines and Motors*: *Structure and Bonding*; Sauvage, J.-P., Ed.; Springer: Berlin, 2001;Vol. 99. (j) Venturi, M.; Credi, A.; Balzani, V. *Molecular Devices and Machines—A Journey into the Nanoworld*, Wiley-VCH: Weinheim, 2003.

(6) "Co-conformation" refers to the relative positions of the mechanically interlocked components with respect to each other, see: Fyfe, M. C. T.; Glink, P. T.; Menzer, S.; Stoddart, J. F.; White, A. J. P.; Williams, D. J. *Angew. Chem., Int. Ed. Engl.* **1997**, *36*, 2068−2070. Energy differences between two translational isomers or co-conformations of greater than 1.18 kcal mol^{-1} imply >90% station occupancy for the more favored site at 298 K.

(7) For examples of chemically responsive molecular shuttles, see: (a) Lane, A. S.; Leigh, D. A.; Murphy, A. *J. Am. Chem. Soc.* **1997**, *119*, 11092−11093. (b) Martínez-Díaz, M.-V.; Spencer, N.; Stoddart, J. F. *Angew. Chem., Int. Ed. Engl.* **1997**, *36*, 1904−1907. (c) Gong, C.; Gibson, H. W. *Angew. Chem., Int. Ed. Engl.* **1997**, *36*, 2331−2333. (d) Ashton, P. R.; Ballardini, R.; Balzani, V.; Baxter, I.; Credi, A.; Fyfe, M. C. T.; Gandolfi, M. T.; Gómez-López, M.; Martínez-Díaz, M.-V.; Piersanti, A.; Spencer, N.; Stoddart, J. F.; Venturi, M.; White, A. J. P.; Williams, D. J. *J. Am. Chem. Soc.* **1998**, *120*, 11932−11942. (e) Jiménez, M. C.; Dietrich-Buchecker, C.; Sauvage, J.-P *Angew. Chem., Int. Ed.* **2000**, *39*, 3284−3287. (f) Lee, J. W.; Kim, K.; Kim, K. *Chem. Commun.* **2001**, 1042−1043. (g) Elizarov, A. M.; Chiu, S.-H.; Stoddart, J. F. *J. Org. Chem.* **2002**, *67*, 9175−9181. (h) Jimenez-Molero, M. C.; Dietrich-Buchecker, C.; Sauvage, J.-P. *Chem. Eur. J.* **2002**, *8*, 1456−1466. (i) Da Ross, T.; Guldi, D. M.; Farran Morales, A.; Leigh, D. A.; Prato, M.; Turco, R. *Org. Lett.* **2003**, *5*, 689−691. (j) Tseng, H.-R.; Vignon, S. A.; Stoddart, J. F. *Angew. Chem., Int. Ed.* **2003**, *42*, 1491−1495.

(8) For examples of photochemically responsive molecular shuttles, see: (a) Benniston, A. C. *Chem. Soc. Rev.* **1996**, *25*, 427−435. (b) Murakami, H.; Kawabuchi, A.; Kotoo, K.; Kunitake, M.; Nakashima, N. *J. Am. Chem. Soc.* **1997**, *119*, 7605−7606. (c) Blanco, M.-J.; Jiménez, M. C.; Chambron, J.-C.; Heitz, V.; Linke, M.; Sauvage, J.-P *Chem. Soc. Rev.* **1999**, *28*, 293−305. (d) Ashton, P. R.; Ballardini, R.; Balzani, V.; Credi, A.; Dress, K. R.; Ishow, E.; Kleverlaan, C. J.; Kocian, O.; Preece, J. A.; Spencer, N.; Stoddart, J. F.; Venturi, M.; Wenger, S. *Chem. Eur. J.* **2000**, *6*, 3558−3574. (e) Wurpel, G. W. H.; Brouwer, A. M.; van Stokkum, I. H. M.; Farran, A.; Leigh, D. A. *J. Am. Chem. Soc.* **2001**, *123*, 11327−11328. (f) Brouwer, A. M.; Frochot, C.; Gatti, F. G.; Leigh, D. A.; Mottier, L.; Paolucci, F.; Roffia, S.; Wurpel, G. W. H. *Science* **2001**, *291*, 2124−2128. (g) Stanier, C. A.; Alderman, S. J.; Claridge, T. D. W.; Anderson, H. L. *Angew. Chem., Int. Ed.* **2002**, *41*, 1769−1772. (h) Altieri, A.; Bottari, G.; Dehez, F.; Leigh, D. A.; Wong, J. K. Y.; Zerbetto, F. *Angew. Chem., Int. Ed.* **2003**, *42*, in press.

(9) For examples of electrochemically responsive molecular shuttles, see ref 8a and the following: (a) Bissell, R. A.; Córdova, E.; Kaifer, A. E.; Stoddart, J. F. *Nature* **1994**, *369*, 133−136. (b) Anelli, P.-L.; Asakawa, M.; Ashton, P. R.; Bissell, R. A.; Clavier, G.; Górski, R.; Kaifer, A. E.; Langford, S. J.; Mattersteig, G.; Menzer, S.; Philp, D.; Slawin, A. M. Z.; Spencer, N.; Stoddart, J. F.; Tolley, M. S.; Williams, D. J. *Chem. Eur. J.* **1997**, *3*, 1113−1135. (c) Collin, J.-P.; Gaviña, P.; Sauvage, J.-P. *New J. Chem.* **1997**, *21*, 525−528. (d) Armaroli, N.; Balzani, V.; Collin, J.-P.; Gaviña, P.; Sauvage, J.-P.; Ventura, B. *J. Am. Chem. Soc.* **1999**, *121*, 4397−4408. (e) Ballardini, R.; Balzani, V.; Dehaen, W.; Dell'Erba, A. E.; Raymo, F. M.; Stoddart, J. F.; Venturi, M. *Eur. J. Org. Chem.* **2000**, 591−602.

(10) For examples of the use of electrical and electrochemical stimuli to control ring rotation in catenanes, catenates, and rotaxanes, see: (a) Amabilino, D. B.; Dietrich-Buchecker, C. O.; Livoreil, A.; Pérez-García, L.; Sauvage, J.-P.; Stoddart, J. F. *J. Am. Chem. Soc.* **1996**, *118*, 3905−3913. (b) Cárdenas, D. J.; Livoreil, A.; Sauvage, J.-P. *J. Am. Chem. Soc.* **1996**, *118*, 11980−11981. (c) Livoreil, A.; Sauvage, J.-P.; Armaroli, N.; Balzani, V.; Flamigni, L.; Ventura, B. *J. Am. Chem. Soc.* **1997**, *119*, 12114−12124. (d) Asakawa, M.; Ashton, P. R.; Balzani, V.; Credi, A.; Hamers, C.; Mattersteig, G.; Montalti, M.; Shipway, A. N.; Spencer, N.; Stoddart, J. F.; Tolley, M. S.; Venturi, M.; White, A. J. P.; Williams, D. J. *Angew. Chem., Int. Ed. Engl.* **1998**, *37*, 333−337. (e) Raehm, L.; Kern, J.-M.; Sauvage, J.-P. *Chem. Eur. J.* **1999**, *5*, 3310−3317. (f) Collier, C. P.; Mattersteig, G.; Wong, E. W.; Luo, Y.; Beverly, K.; Sampaio, J.; Raymo, F. M.; Stoddart, J. F.; Heath, J. R. *Science* **2000**, *289*, 1172−1175. (g) Asakawa, M.; Higuchi, M.; Mattersteig, G.; Nakamura, T.; Pease, R.; Raymo, F. M.; Shimizu, T.; Stoddart, J. F. *Adv. Mater.* **2000**, *12*, 1099−1102. (h) Bermudez, V.; Capron, N.; Gase, T.; Gatti, F. G.; Kajzar, F.; Leigh, D. A.; Zerbetto, F.; Zhang, S. *Nature* **2000**, *406*, 608−611. (i) Ashton, P. R.; Baldoni, V.; Balzani, V.; Credi, A.; Hoffmann, H. D. A.; Martínez-Díaz, M.-V.; Raymo, F. M.; Stoddart, J. F.; Venturi, M. *Chem. Eur. J.* **2001**, *7*, 3482−3493.

(11) For examples of the use of electrochemical stimuli to control threading and dethreading in pseudorotaxanes and other host−guest systems, see: (a) Bernardo, A. R.; Stoddart, J. F.; Kaifer, A. E. *J. Am. Chem. Soc.* **1992**, *114*, 10624−10631. (b) Collin, J.-P.; Gaviña, P.; Sauvage, J.-P. *Chem. Commun.* **1996**, 2005−2006. (c) Asakawa, M.; Ashton, P. R.; Balzani, V.; Credi, A.; Mattersteig, G.; Matthews, O. A.; Montalti, M.; Spencer, N.; Stoddart, J. F.; Venturi, M. *Chem. Eur. J.* **1997**, *3*, 1992−1996. (d) Devonport, W.; Blower, M. A.; Bryce, M. R.; Goldenberg, L. M. *J. Org. Chem.* **1997**, *62*, 885−887. (e) Credi, A.; Montalti, M.; Balzani, V.; Langford, S. J.; Raymo, F. M.; Stoddart, J. F. *New. J. Chem.* **1998**, *22*, 1061−1065. (f) Asakawa, M.; Ashton, P. R.; Balzani, V.; Boyd, S. E.; Credi, A.; Mattersteig, G.; Menzer, S.; Montalti, M.; Raymo, F. M.; Ruffilli, C.; Stoddart, J. F.; Venturi, M.; Williams, D. J. *Eur. J. Org. Chem.* **1999**, 985−994. (g) Ashton, P. R.; Balzani, V.; Becher, J.; Credi, A.; Fyfe, M. C. T.; Mattersteig, G.; Menzer, S.; Nielsen, M. B.; Raymo, F. M.; Stoddart, J. F.; Venturi, M.; Williams, D. J. *J. Am. Chem. Soc.* **1999**, *121*, 3951−3957. (h) Cooke, G.; Duclairoir, F. M. A.; Rotello, V. M.; Stoddart, J. F. *Tetrahedron Lett.* **2000**, *41*, 8163−8166. (i) Balzani, V.; Credi, A.; Mattersteig, G.; Matthews, O. A.; Raymo, F. M.; Stoddart, J. F.; Venturi, M.; White, A. J. P.; Williams, D. J. *J. Org. Chem.* **2000**, *65*, 1924−1936. (j) Balzani, V.; Becher, J.; Credi, A.; Nielsen, M. B.; Raymo, F. M.; Stoddart, J. F.; Talarico, A. M.; Venturi, M. *J. Org. Chem.* **2000**, *65*, 1947−1956. (k) Lahav, M.; Shipway, A. N.; Willner, I.; Nielsen, M. B.; Stoddart, J. F. *J. Electroanal. Chem.* **2000**, *482*, 217−221.

(12) Earlier attempts to make redox-active hydrogen-bonded molecular shuttles based on anthraquinone subunits were unsuccessful (Dunnett, J. A. Ph.D. Thesis, University of Manchester Institute of Science and Technology, U.K., 2000).

Chart 1. Molecular Shuttle **1**, Shown as the *succ*-**1** Positional Isomer, and Thread **2**[a]

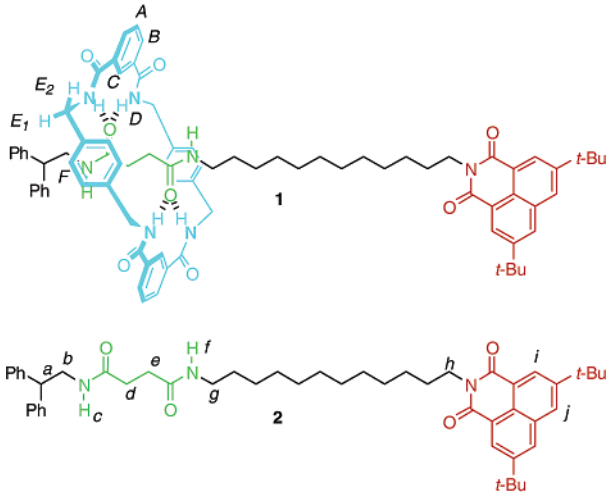

[a] The letters indicate selected nonequivalent ^{1}H environments.

properties. Electrochemistry is also advantageous in this regard since the same stimulus can simultaneously act as both effector and detector of the motion.

Here we report the cyclic voltammetry of **1** and a series of related rotaxanes and threads. The rates and energies obtained from the electrochemical redox experiments are consistent with those obtained photochemically. The spectroscopic and electrochemical behavior of key model compounds is used to show unambiguously that the dynamics observed is a consequence of the position of the macrocycle on the thread changing upon reduction of the naphthalimide unit.

Design

Hydrogen bonds are largely electrostatic in nature,[13] so changes in the electron charge density of a hydrogen-bonding group can have a dramatic effect on its binding ability—a phenomenon exploited in redox-switched molecular recognition[14] and the modulation of protein and peptide structure.[15] Molecular shuttle **1** consists of a benzylic amide macrocycle—a strong hydrogen-bond donor through the amide NH groups—mechanically linked onto a thread molecule, **2**, containing two potential hydrogen-bond acceptor moieties—a succinamide (*succ*) station and a redox-active 3,6-di-*tert*-butyl-1,8-naphthalimide[16] (*ni*) station—separated by a C_{12} aliphatic spacer (Chart 1). The ability of the *succ* station to template formation of the macrocycle by a five-component 'clipping' reaction between isophthaloyl dichloride and *p*-xylylene diamine in apolar solvents is well established.[8f] X-ray crystal structures of model succinamide rotaxanes **3** and **4** (Figures 2 and 3) demonstrate an excellent fit between the thread and macrocycle, both in terms of steric interactions and the complementary positioning of the hydrogen-bonding amide groups on the two components. While the structure of **3** shows both intra- and intermolecular hydrogen bonding in the solid state, **4** has a solely intramolecularly hydrogen-bonded structure and is presumably more representative of the hydrogen-bonding motifs adopted by 'isolated' molecules in solution. The macrocycle adopts a near-perfect chair conformation, driven by formation of two sets of bifurcated hydrogen bonds between the amide protons of each isophthalamide moiety and the succinamide carbonyl oxygens.

The choice of a substituted naphthalimide unit as the redox-active station was inspired by the work of Smith[14b] and Rotello.[14c,e,f] Imides are comparatively poor hydrogen-bond acceptors;[17] indeed, threads containing just the naphthalimide

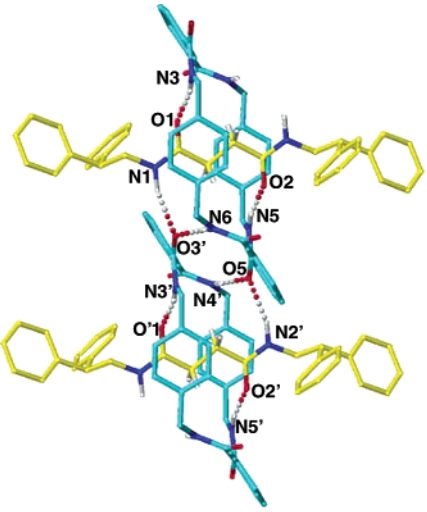

Figure 2. X-ray crystal structure of [2]rotaxane **3** (for clarity carbon atoms of the macrocycle are shown in blue and the carbon atoms of the thread are shown in yellow; oxygen atoms are depicted in red, nitrogen atoms in dark blue, and amide protons in white). Intramolecular hydrogen-bond distances (Å): O1−HN3/O2−HN5 1.88. Intermolecular hydrogen-bond distances (Å): O5−HN4′/ O3′-HN6 2.0, O3′-HN1/O5−HN2′ 2.21.

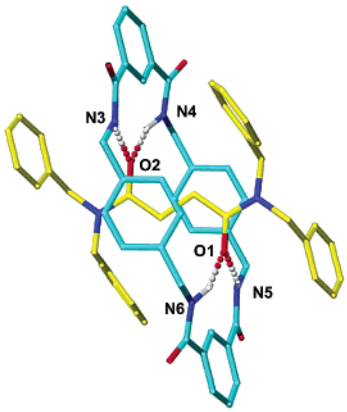

Figure 3. X-ray crystal structure of [2]rotaxane **4**. Intramolecular hydrogen-bond distances (Å): O2−HN3/O1−HN5 1.90, O2−HN4/O1−HN6 2.01.

(13) Morokuma, K. *Acc. Chem. Res.* **1977**, *10*, 294−300.
(14) See, for example: (a) Brooksby, P. A.; Hunter, C. A.; McQuillan, A. J.; Purvis, D. H.; Rowan, A. E.; Shannon, R. J.; Walsh, R. *Angew. Chem., Int. Ed. Engl.* **1994**, *33*, 2489−2491. (b) Ge, Y.; Lilienthal, R.; Smith, D. K. *J. Am. Chem. Soc.* **1996**, *118*, 3976−3977. (c) Deans, R.; Niemz, A.; Breinlinger, E. C.; Rotello, V. M. *J. Am. Chem. Soc.* **1997**, *119*, 10863−10864. (d) Boulas, P. L.; Gómez-Kaifer, M.; Echegoyen, L. *Angew. Chem., Int. Ed. Engl.* **1998**, *37*, 216−247. (e) Niemz, A.; Rotello, V. M. *Acc. Chem. Res.* **1999**, *32*, 44−52. (f) Boal, A. K.; Rotello, V. M. *J. Am. Chem. Soc.* **1999**, *121*, 4914−4915. (g) Ge, Y.; Miller, L.; Ouimet, T.; Smith, D. K *J. Org. Chem.* **2000**, *65*, 8831−8838. (h) Ge, Y.; Smith, D. K. *Anal. Chem.* **2000**, *72*, 1860−1865. (i) Carr, J. D.; Coles, S. J.; Hursthouse, M. B.; Light, M. E.; Tucker, J. H. R.; Westwood, J. *Angew. Chem., Int. Ed.* **2000**, *39*, 3296−3299. (j) Tucker, J. H. R.; Collinson, S. R. *Chem. Soc. Rev.* **2002**, *31*, 147−156. (k) Cooke, G.; Rotello, V. M. *Chem. Soc. Rev.* **2002**, *31*, 275−286.
(15) See, for example: (a) Schenck, H. L.; Dado, G. P.; Gellman, S. H. *J. Am. Chem. Soc.* **1996**, *118*, 12487−12494. (b) Pascher, T.; Chesick, J. P.; Winkler, J. R.; Gray, H. B. *Science* **1996**, *271*, 1558−1560.
(16) The *tert*-butyl substituents provide the steric bulk necessary to stopper the rotaxane while only slightly altering the redox potential of the naphthalimide group ($E_{1/2}$ (**2**) = −1.41 V cf. $E_{1/2}$ (*N*-methyl naphthalimide) = −1.31 V): Viehbeck, A.; Goldberg, M. J.; Kovac, C. A. *J. Electrochem. Soc.* **1990**, *137*, 1460−1466.
(17) Jeffrey, G. A. *An Introduction to Hydrogen Bonding*; Oxford University Press: New York, 1997.

Chart 2. Model Rotaxanes **3**−**8** Shown as the *succ*- Positional Isomers[a]

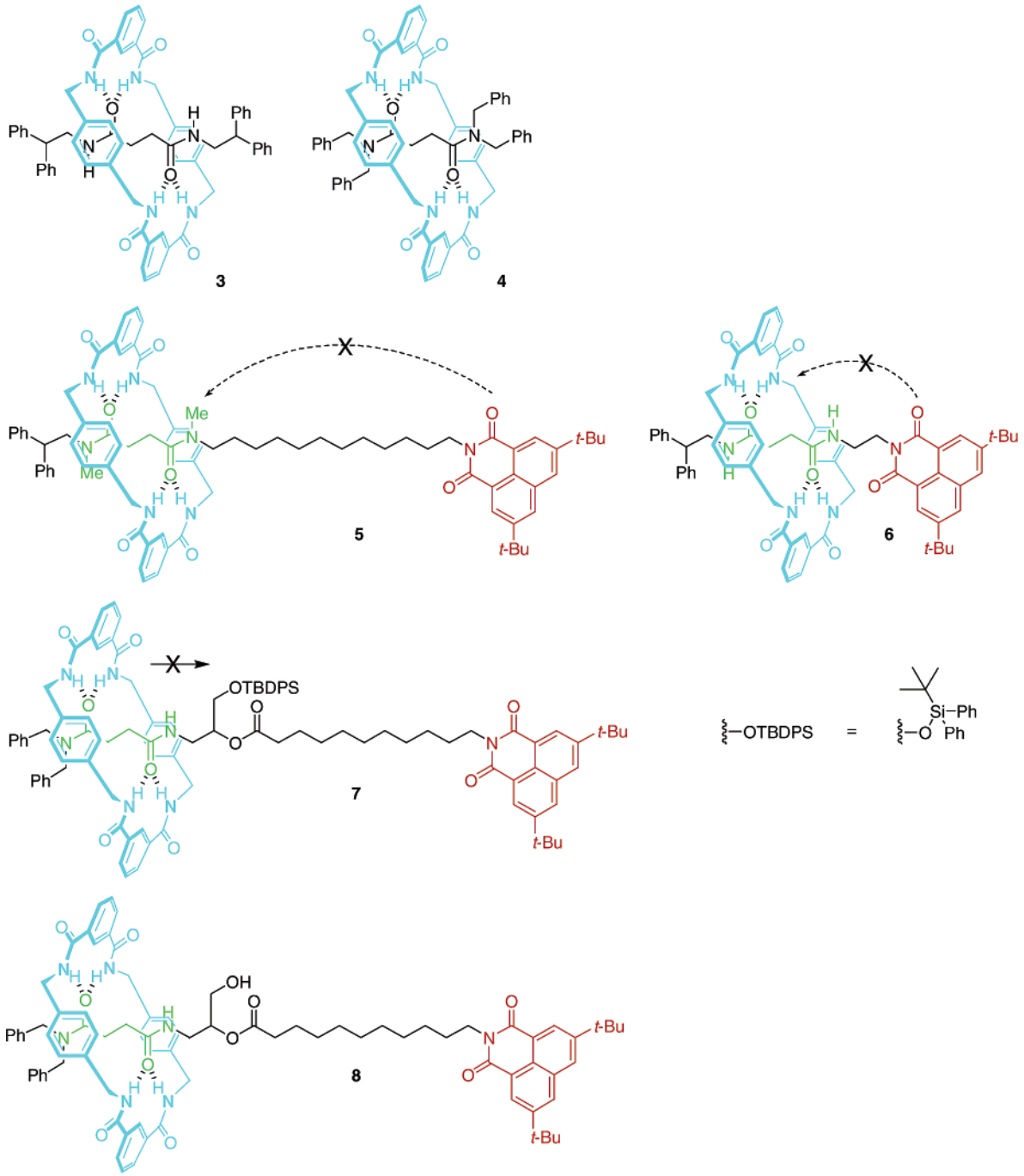

[a] The dashed lines show hydrogen-bond interactions possible in **1** but disallowed in the model compound. Solid lines show changes of co-conformation that require shuttling which are disallowed in the model compound.

unit do not template formation of the benzylic amide macrocycle to give rotaxanes. To minimize its free energy, the macrocycle in **1** must therefore sit over the succinamide station in non-hydrogen-bonding solvents, so that co-conformation *succ*-**1** predominates (Figure 4). One-electron reduction of naphthalimides to the corresponding radical anion, however, results in a substantial increase in electron charge density on the imide carbonyls and a concomitant increase in hydrogen-bond accepting ability.[14b,c,e] In **1**, this change in oxidation state should reverse the relative hydrogen-bonding abilities of the two thread stations so that co-conformation *ni*-$\mathbf{1}^{-\bullet}$ is preferred in the reduced state. This dynamic process was studied in **1** through cyclic voltammetry experiments and ^{1}H NMR spectroscopy. To probe the nature of the stimulated motion, we carried out similar studies on model rotaxanes **5**−**8** (Chart 2). Each of these analogues of **1** is designed to restrict a different type of conformational or co-conformational change so that the true origin of the effects seen for **1** could be unambiguously determined.

Synthesis

Rotaxanes **1**, **5,** and **6** were prepared according to Scheme 1. Treatment of threads **2**, **9,** or **10** with 10 equiv of each of *p*-xylylene diamine and isophthaloyl dichloride ($CHCl_3$, Et_3N,

Scheme 1. Synthesis of Rotaxanes **1**, **5,** and **6**[a]

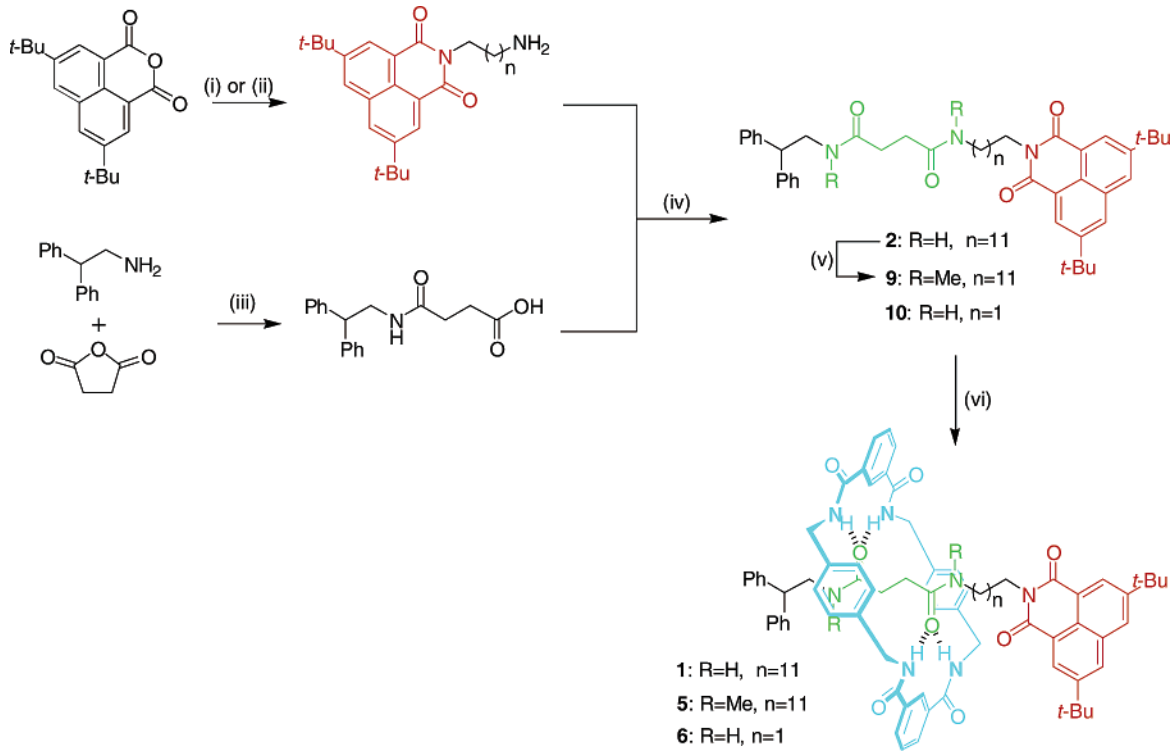

[a] (i) 1,12-Diaminododecane, Et_3N, EtOH, Δ, 14%; (ii) 1,2-ethylenediamine, EtOH, Δ, 78%; (iii) pyridine, AcOH, 90%; (iv) 1-[3-(dimethylamino)propyl]-3-ethylcarbodiimide hydrochloride (EDCI), 4-(dimethylamino)pyridine (DMAP), CH_2Cl_2, 0 °C to RT, 98% (**2**), 93% (**10**); (v) MeI, NaH, THF, 0 °C to RT, 94%; (vi) isophthaloyl dichloride, *p*-xylylene diamine, Et_3N, $CHCl_3$, 59% (**1**), 33% (**5**), 62% (**6**).

Scheme 2. Synthesis of Rotaxanes **7** and **8**[a]

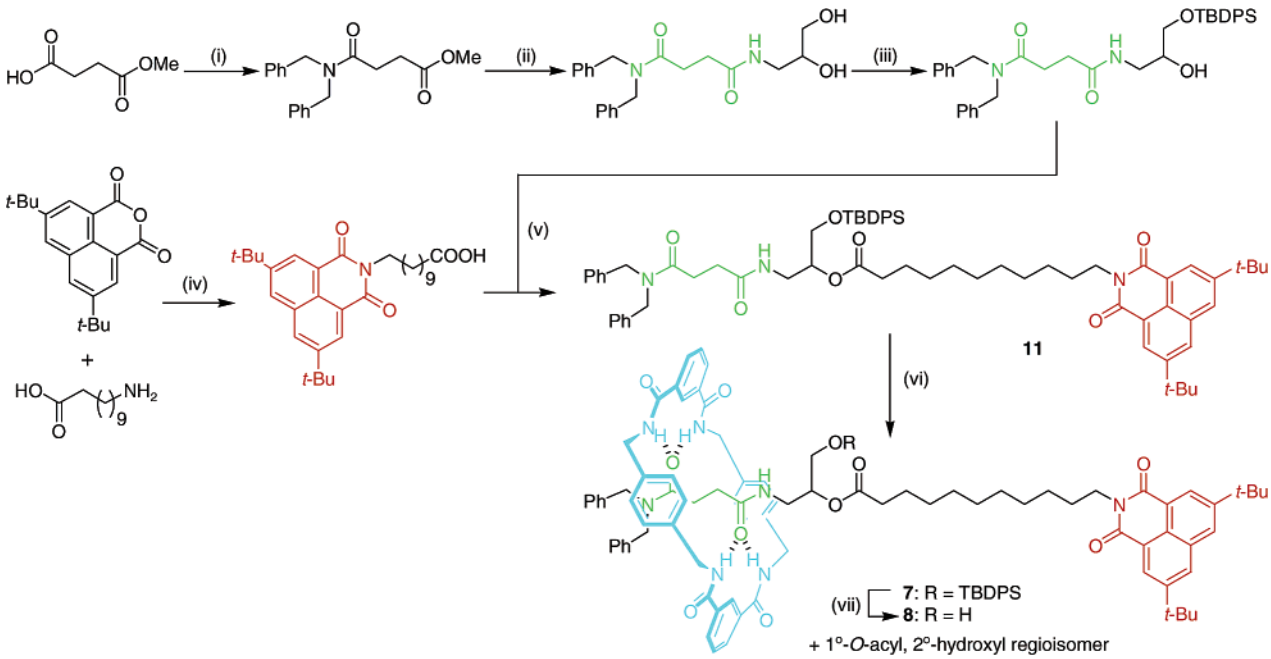

[a] (i) $(PhCH_2)_2NH$, EDCI, DMAP, CH_2Cl_2, 0 °C to RT, 94%; (ii) 3-amino-propane-1,2-diol, Δ, 84%; (iii) *tert*-butylchlorodiphenylsilane (TBDPSCl), imidazole, DMAP, CH_2Cl_2, 62%; (iv) pyridine, Δ, 60%; (v) EDCI, DMAP, CH_2Cl_2, 0 °C to RT, 90%; (vi) isophthaloyl dichloride, *p*-xylylene diamine, Et_3N, $CHCl_3$, 23%; (vii) CH_2Cl_2, tetrabutylammonium fluoride (TBAF), 70%.

4 h, high dilution) provided [2]rotaxanes **1**, **5,** and **6** in 59%, 33%, and 62% yields, respectively. Scheme 2 shows the synthesis of 'gate-closed' thread **11** which, under similar rotaxane-forming conditions, furnished [2]rotaxane **7** in 23% yield. The 'gate-opened' rotaxane **8** was obtained by treatment of **7** with a stoichiometric amount of tetra-*n*-butylammonium fluoride in CH_2Cl_2.[18]

(18) 'Gate-opened' rotaxane **8** was obtained together with the 1°-*O*-acyl, 2°-hydroxyl regioisomer from which it was not separated.

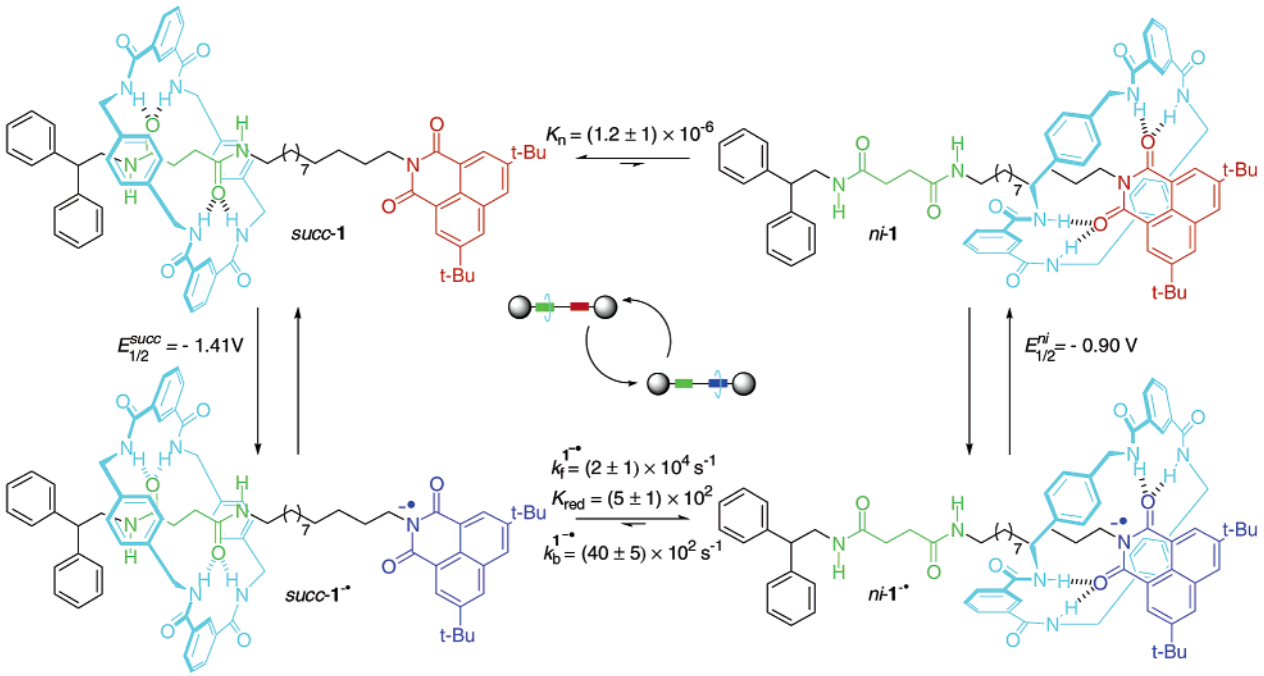

Figure 4. An electrochemically switchable, hydrogen-bonded molecular shuttle **1**. In the neutral state, the translational co-conformation *succ*-**1** is predominant as the *ni* station is a poor hydrogen-bond acceptor ($K_n = (1.2 \pm 1) \times 10^{-6}$). Upon reduction, the equilibrium between *succ*-**1**$^{-\bullet}$ and *ni*-**1**$^{-\bullet}$ is altered ($K_{red} = (5 \pm 1) \times 10^2$) because *ni*$^{-\bullet}$ is a powerful hydrogen-bond acceptor. Upon reoxidation, the macrocycle shuttles back to its original position. Repeated reduction and oxidation causes the macrocycle to shuttle forward and backward between the two stations. All the values shown refer to experiments in anhydrous THF at 298 K with tetrabutylammonium hexafluorophosphate as the supporting electrolyte.

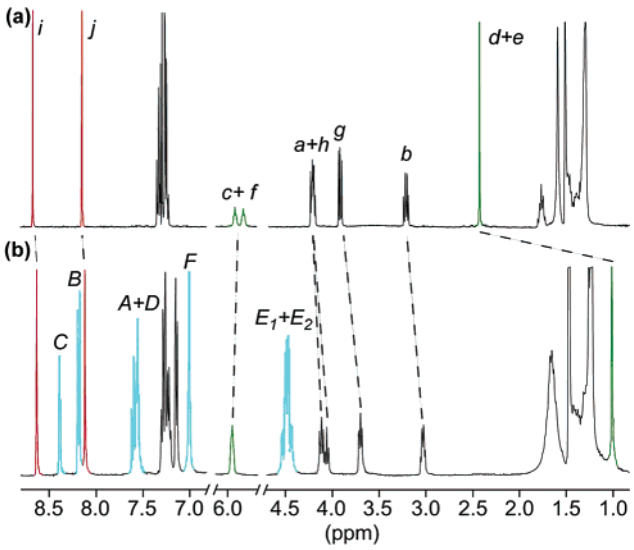

Figure 5. ^{1}H NMR spectra (400 MHz) of (a) **2** and (b) **1** in $CDCl_3$ at 298 K. The letters correspond to the assignments shown in Chart 1.

Co-conformation in the Neutral State

^{1}H NMR spectroscopy is a useful tool for studying translational isomerism in rotaxanes. For benzylic amide macrocycle-containing rotaxanes, aromatic ring currents in the *p*-xylylene rings result in significant upfield shifting (typically $\Delta\delta_H > 1$ ppm) for protons on the portion of the thread covered by the macrocycle.[19] Comparison of the ^{1}H NMR spectra of rotaxane **1** and the corresponding thread **2** in $CDCl_3$ (Figure 5) shows such an upfield shift for succinic methylene protons H_d and H_e ($\Delta\delta_H = -1.45$ ppm).[20] Protons in close proximity to the *succ* station (H_a, H_b, and H_g) are also shielded but to a lesser extent; all other thread protons, including those of the naphthalimide, are essentially unaffected by the presence of the macrocycle. The infrared spectrum of **1** in $CHCl_3$ also shows no changes in the CO stretching band of the naphthalimide moiety compared to the spectrum of **2** ($\nu_{CO_{stretch}} = 1780\ cm^{-1}$ in each case), suggesting no significant hydrogen bonding occurs to the naphthalimide subunit in the rotaxane.[8f] Clearly the *succ*-**1** translational isomer is the predominant structure in chloroform.

Table 1. Solvent Effects on Chemical Shifts (δ_H) and Differential Chemical Shifts ($\Delta\delta_H$) for Succinamide Protons in **1** and **2**

	NH_c and NH_f		H_d and H_e
solvent	δH (**1**)/ppm	δH (**2**)/ppm	$\Delta\delta$H/ppm
$CDCl_3$	5.95	5.73; 5.61	−1.45
d_3-MeCN[a]	6.47; 6.42	6.42; 4.22	−1.2
d_8-THF	7.84; 7.63	7.20; 7.12	−1.2
d_6-DMSO	7.92; 7.40	7.78; 7.60	−0.7

[a] Spectra collected at 329 K due to low solubility of **1** in d_3-MeCN.

In fact, unlike peptide-based molecular shuttles,[7a] the positional integrity of the macrocycle in **1** is remarkably independent of the nature of the solvent. The difference in chemical shifts for methylene protons H_d and H_e in **1** and **2** as well as the shifts for succinamide amide protons H_c and H_f in solvents of varying hydrogen-bonding ability are shown in Table 1. The increasing δ_H values for the amide protons illustrate the ability of these solvents to disrupt hydrogen bonding ($CDCl_3$ < d_3-MeCN < d_8-THF < d_6-DMSO). It can be seen, however, that in $CDCl_3$, d_3-MeCN, and d_8-THF, shielding of the *succ* methylene protons is virtually unchanged, indicating that positional integrity of the

(19) Johnston, A. G.; Leigh, D. A.; Murphy, A.; Smart, J. P.; Deegan, M. D. *J. Am. Chem. Soc.* **1996**, *118*, 10662−10663.

(20) Dilution experiments demonstrated that intermolecular hydrogen-bonding interactions were absent at concentrations of 10 mmol L^{-1} and below for the current rotaxanes and threads. All NMR spectra discussed were therefore collected at this standard concentration.

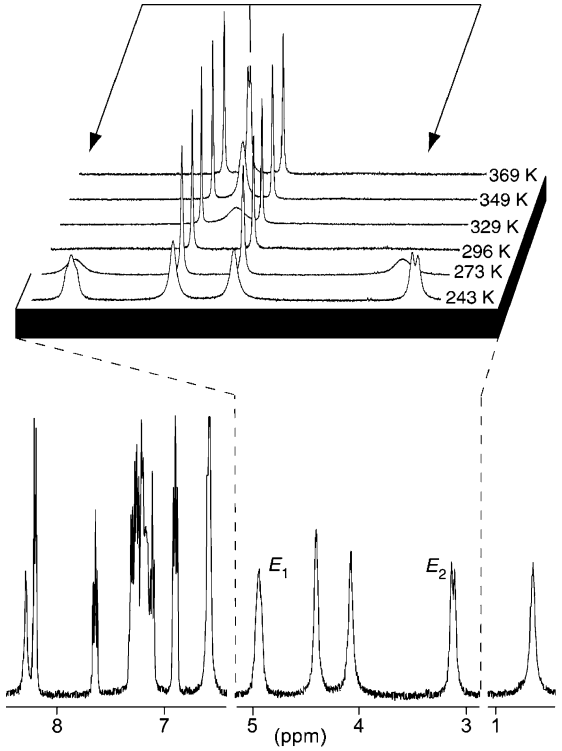

Figure 6. ^{1}H NMR spectrum of **4** (400 MHz, $CDCl_3$) at 243 K showing slow pirouetting of the macrocycle about the thread (H_{E1} and H_{E2} resolved). SPT-SIR between resolved signals gives the energy barrier for macrocycle pirouetting. Higher temperature spectra (expansion, 243−296 K ($CDCl_3$) and 329−369 K ($C_2D_2Cl_4$)) illustrate the wide temperature ranges that can exist between full resolution and coalescence of signals affected by the dynamic processes.

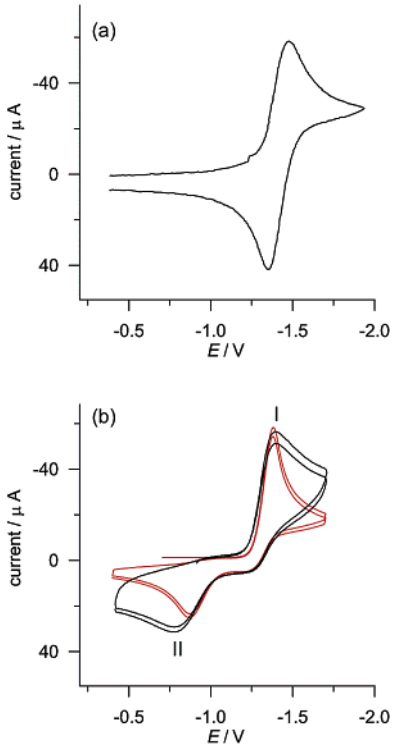

Figure 7. Cyclic voltammograms at 298 K of (a) **2** and (b) **1** showing both experimental (black line) and simulated (red line) results. Experiments carried out on 1 mmol L^{-1} solutions of substrate in anhydrous THF with tetrabutylammonium hexafluorophosphate (5×10^{-2} mol L^{-1}) as electrolyte and ferrocene as internal standard. Scan rate: 2 V s^{-1}. Working electrode: Pt.

shuttle is maintained in all three solvents. Even in d_6-DMSO the upfield shift for H_d and H_e is only reduced by ≈50%, indicating that even in this strongly hydrogen-bond-disrupting solvent the macrocycle still spends a significant amount of time over the *succ* station.

The energy barrier for pirouetting of the macrocycle around the thread provides a definitive measure of the strength of the intercomponent interactions.[21] Due to the complexity of the ^{1}H NMR spectra of **1** and its analogues, this process was studied in the simpler, C_2-symmetric, rotaxanes **3** and **4** as models for shuttles **1** and **5**, respectively. Variable-temperature (VT) ^{1}H NMR experiments in $CDCl_3$ and $C_2D_2Cl_4$ (because of the wide temperature range involved) using both the coalescence method[22] and spin polarization transfer by selective inversion recovery (SPT-SIR)[23] were employed to calculate the rates of macrocycle pirouetting. The VT ^{1}H NMR plot for **4** (Figure 6) shows the signals for macrocycle benzylic methylene protons E_1 and E_2 are well separated at 243 K, while a single sharp peak is observed at 369 K.[24] SPT-SIR of **4** gives an energy barrier for macrocycle pirouetting at 298 K of 12.9 ± 0.1 kcal mol^{-1}. Similarly, the barrier for **3** was determined as 11.2 ± 0.1 kcal mol^{-1} at 298 K. Even when compared to the fumaramide template which holds the hydrogen-bond acceptor groups of the thread in a close-to-ideal arrangement for the donor groups in the macrocycle ($\Delta G_{298}^{\ddagger}$ for the fumaramide analogue of **3** = 13.4 ± 0.1 kcal mol^{-1})[21b] it can be seen that the succinic templates in **3** and **4** result in strong intercomponent hydrogen bonding. Clearly, dissociation from the succinamide station in a molecular shuttle will involve a significant energy barrier.

Redox-Switched Shuttling

Translocation of the macrocycle in **1** could be readily triggered by electrochemical reduction of the naphthalimide station to its radical anion. Since the changes in hydrogen-bonding pattern affect the electrochemical properties of the system, the shuttling process could be both effected and observed in cyclic voltammetry (CV) experiments of **1** and its analogues and components.[25] The CV response of **2** in anhydrous THF (Figure 7a) exhibits a reversible, one-electron reduction peak corresponding to reduction and reoxidation of the naphthalimide group (**2**/**2**$^{-\bullet}$, $E_{1/2} = -1.41$ V).[16] Rotaxane **1**, on the other hand, displays a similar cathodic signal, **I** (E_c =

(21) For examples of macrocycle pirouetting in benzylic amide macrocycle-based [2]rotaxanes, see ref 10h and the following: (a) Leigh, D. A.; Murphy, A.; Smart, J. P.; Slawin, A. M. Z. *Angew. Chem., Int. Ed. Engl.* **1997**, *36*, 728−732. (b) Gatti, F. G.; Leigh, D. A.; Nepogodiev, S. A.; Slawin, A. M. Z.; Teat, S. J.; Wong, J. K. Y. *J. Am. Chem. Soc.* **2001**, *121*, 5983−5989. (c) Gatti, F. G.; León, S.; Wong, J. K. Y.; Bottari, G.; Altieri, A.; Farran Morales, A. M.; Teat, S. J.; Frochot, C.; Leigh, D. A.; Brouwer, A. M.; Zerbetto, F. *Proc. Natl. Acad. Sci. U.S.A.* **2003**, *100*, 10−14.

(22) Sandström, J. *Dynamic NMR Spectroscopy*; Academic Press: London, 1982.

(23) Dahlquist, F. W.; Longmur, K. J.; Du Vernet, R. B. *J. Magn. Reson.* **1975**, *17*, 406−413. For applications of SPT-SIR to dynamic processes in rotaxanes, see, for example: Clegg, W.; Gimenez-Saiz, C.; Leigh, D. A.; Murphy, A.; Slawin, A. M. Z.; Teat, S. J. *J. Am. Chem. Soc.* **1999**, *121*, 4124−4129. For an example of how the SPT-SIR experiments were performed for the current systems, see the Supporting Information.

(24) Due to the wide temperature range, spectra were collected in $CDCl_3$ from 243 to 296 K and in $C_2D_2Cl_4$ from 329 to 369 K

(25) Cyclic voltammetry was carried out on 10^{-3} mol L^{-1} solutions of substrate in anhydrous THF with tetrabutylammonium hexafluorophosphate (TBHF, 5×10^{-2} mol L^{-1}) as electrolyte and ferrocene as internal standard. The invariance of the chemical shift for amide protons of **1** and **2** in d_8-THF in the presence of TBHF at 5×10^{-2} mol L^{-1} suggests that the electrolyte does not significantly affect amide−amide intramolecular hydrogen bonds at these concentrations.

−1.40 V, at 2 V s^{-1}), yet lacks the corresponding oxidation peak (Figure 7b). Rather, a new one-electron anodic peak, **II**, appears toward more positive potentials ($E_a = -0.89$ V, at 2 V s^{-1}). On subsequent scans, performed without renewal of the diffusion layer, it is only these two peaks that appear, indicating that the system returns to its original state after each cycle on this time scale.

These results can be interpreted in terms of a standard square scheme for a redox-switched binding process whereby the reversible translational isomerism equilibria for each oxidation state are connected via the electron-transfer steps (Figure 4). As shown earlier, the shuttle in its neutral state overwhelmingly adopts co-conformation *succ*-**1**. Reduction of the naphthalimide group to give *succ*-**1**$^{-\bullet}$ is therefore unaffected by the macrocycle. Due to the increased hydrogen-bonding ability of naphthalimide in its reduced state, the equilibrium between co-conformations in this oxidation state lies far toward the *ni*-**1**$^{-\bullet}$ isomer so that shuttling of the macrocycle occurs. Resultant hydrogen bonding to the macrocycle amide protons stabilizes the increased electron charge on the naphthalimide so that more positive potentials must be reached before the oxidation *ni*-**1**$^{-\bullet}$ → *ni*-**1** occurs ($\Delta E_p = 0.51$ V). Once again in the neutral state, the macrocycle shuttles back to the preferred succinamide station therefore restoring the system to its original state as *succ*-**1**. The absence of any *succ*-**1**$^{-\bullet}$ → *succ*-**1** oxidation peak or *ni*-**1** → *ni*-**1**$^{-\bullet}$ reduction peak demonstrates the remarkable positional integrity of the shuttle in both oxidation states while also indicating that the shuttling process is rapid on the time scale of the experiment.

The CV curve of **1** was simulated (Figure 7b). Fitting with the experimental results allowed calculation of the redox potential for the electron-transfer process *ni*-**1**$^{-\bullet}$ ⇆ *ni*-**1** as $E_{1/2}^{ni} = -0.90$ V. Also obtained were the rate constants in the reduced state for the forward shuttling process (*succ*-**1**$^{-\bullet}$ → *ni*-**1**$^{-\bullet}$; $k_f^{\mathbf{1}-\bullet} = (2 \pm 1) \times 10^4$ s^{-1}; $T = 298$ K, THF) and the backward process (*ni*-**1**$^{-\bullet}$ → *succ*-**1**$^{-\bullet}$; $k_b^{\mathbf{1}-\bullet} = (40 \pm 5) \times 10^2$ s^{-1}; $T = 298$ K, THF). These figures yield a co-conformational equilibrium constant for the reduced state of $K_{red} = (5 \pm 1) \times 10^2$ confirming that the *ni*-**1**$^{-\bullet}$ co-conformation is indeed strongly preferred. The *ni*-**1** → *succ*-**1** shuttling process occurs faster than the *ni*-**1**$^{-\bullet}$ → *ni*-**1** oxidative electron-transfer step, so that it is not possible to calculate rate constants for this process.[26] The equilibrium constants in each oxidation state for any such redox-switched binding process are related by eq 1.[27] Accordingly, the constant for the neutral state co-conformational equilibrium was calculated as $K_n = (1.2 \pm 1) \times 10^{-6}$,[28] consistent with the predominance of the *succ*-**1** co-conformation shown by ^{1}H NMR and IR.

$$\Delta E^{o} = E_{1/2}^{\ ni} - E_{1/2}^{\ succ} = \frac{RT}{nF}\ln\left(\frac{K_{red}}{K_n}\right) \qquad (1)$$

Given the fast rate constants for shuttling in the reduced state, a scan rate on the order of 10 kV s^{-1} would be required to observe the *succ*-**1**$^{-\bullet}$ → *succ*-**1** oxidation before shuttling to *ni*-**1**$^{-\bullet}$ occurs. Such high scan rates are not achievable with **1** due to the high resistivity of THF solutions. An alternative strategy is to run the experiments at low temperatures to slow the shuttling motion. Indeed, at 213 K, the cathodic peak, **I**, for reduction of the *succ*-**1** species exhibits an anodic counterpart, **III**, while the intensity of anodic peak **II** is correspondingly reduced (Figure 8). The even greater resistivity at this temperature prevents the use of higher scan rates to oxidize all *succ*-**1**$^{-\bullet}$ species before shuttling occurs.

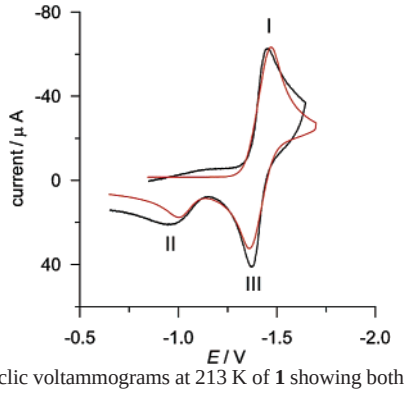

Figure 8. Cyclic voltammograms at 213 K of **1** showing both experimental (black line) and simulated (red line) results. Experiments carried out on 1 mmol L^{-1} solutions of substrate in anhydrous THF with tetrabutylammonium hexafluorophosphate (5×10^{-2} mol L^{-1}) as electrolyte and ferrocene as internal standard. Scan rate: 2 V s^{-1}. Working electrode: Pt.

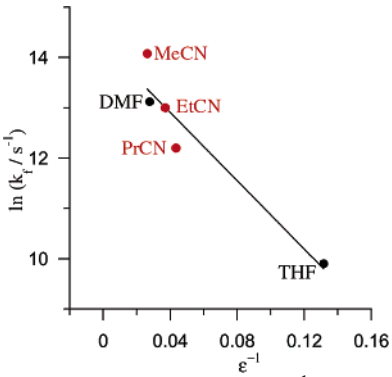

Figure 9. Variation of forward shuttling rate ($k_f^{\mathbf{1}-\bullet}$) with relative permittivity, ϵ, of solvent. Data points in black are calculated from experiments using an electrochemical stimulus; data points in red are calculated from experiments using a photochemical stimulus.[8f] All experiments were carried out at 298 K.

Simulation of the low-temperature CV curve (Figure 8) indicated, as expected, that the rate constant for forward shuttling in the reduced state is much lower than that at room temperature ($k_f^{\mathbf{1}-\bullet} \approx 1$ s^{-1}; $T = 213$ K, THF). By repeating the simulation at various temperatures and subjecting the results to an Eyring plot analysis, the following activation parameters for the shuttling process in the reduced state were obtained: $\Delta H^{\ddagger} = 14.0 \pm 0.6$ kcal mol^{-1}, $\Delta S^{\ddagger} = 8.7 \pm 2$ cal K^{-1} mol^{-1} and $\Delta G_{298}^{\ddagger} = 11.4 \pm 1.2$ kcal mol^{-1}.

The electrochemical results are consistent with the photochemically induced shuttling experiments carried out in alkylnitrile solutions.[8f] Unfortunately, when carrying out the electrochemistry experiments in acetonitrile, adsorption phenomena at the electrodes prevented any analysis of the curves and therefore any direct comparison of the two stimuli in the same solvent. The electrochemical measurements were instead repeated in DMF. Figure 9 compares the forward shuttling rates

(26) On increasing the scan rate from 20 mV s^{-1} to 250 V s^{-1}, the anodic peak II shifts to higher potentials by ≈60 mV/log unit of scan rate, indicating that the oxidation process is kinetically slow. Due to the non-Nernstian nature of the oxidation process, the rate constants relative to the *ni*-**1**/*succ*-**1** shuttling process can therefore not be obtained by fitting of the CV curve. The absence of a cathodic counterpart for peak II at scan rates as high as 250 V s^{-1}, however, allows estimation of $k_b^1 \approx 1.6 \times 10^3$ s^{-1}, so that $k_f^1 \approx 2 \times 10^{-3}$ s^{-1}.

(27) Kaifer, A.; Gómez-Kaifer, M. *Supramolecular Electrochemistry*; Wiley-VCH: Weinheim, 1999.

(28) Assuming $E_{1/2}^{succ} = E_{1/2}$ (**2**) = −1.41 V.

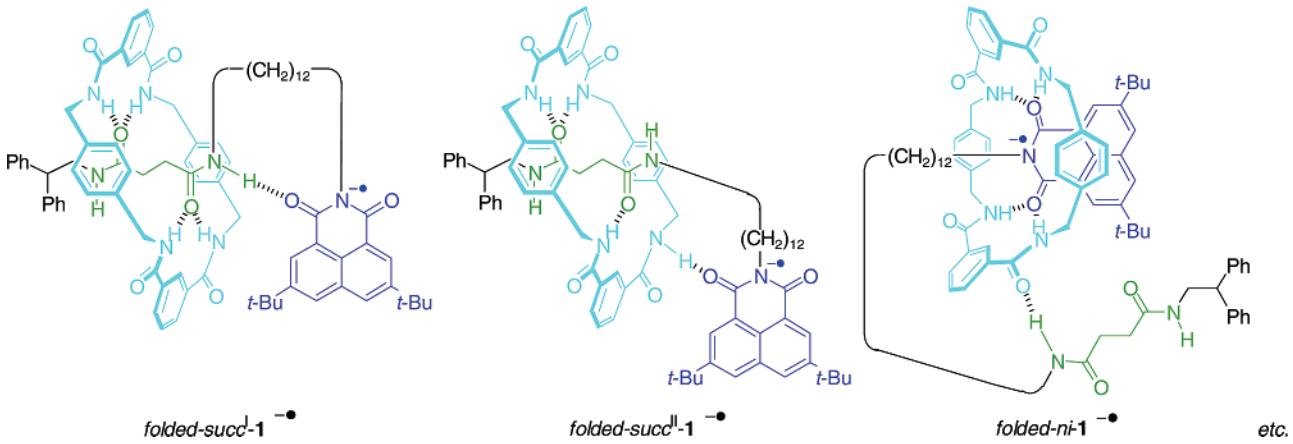

Figure 10. Possible folded co-conformations for reduced rotaxane $\mathbf{1}^{-\bullet}$. In fact, only *folded-ni*-$\mathbf{1}^{-\bullet}$ is a low-energy structure.

calculated from a range of experiments in different solvents using the two stimuli. An approximately linear relationship exists between the rate of shuttling ($k_f^{\mathbf{1}-\bullet}$) and polarity of the medium, suggesting that the nature of the solvent is the main variable affecting the shuttling rates in these experiments (the presence of the supporting electrolytes in the electrochemistry experiments could also play a role, but see ref 25). Pleasingly, the shuttling process in this class of molecular shuttles is independent of the means—light or electrons—used to trigger it.

Is the Redox-Induced Motion Really Shuttling?

It might be argued that hydrogen-bonding interactions between the *ni* station and either the *succ* station or the macrocycle in $\mathbf{1}^{-\bullet}$ could arise from folded conformations (e.g., *folded-succ*^{I}-$\mathbf{1}^{-\bullet}$ and *folded-succ*^{II}-$\mathbf{1}^{-\bullet}$, Figure 10), accounting for the experimental observations without requiring an actual change in the position of the macrocycle on the thread in the reduced rotaxane. To demonstrate unequivocally that the reduction of **1** does, in fact, result in shuttling of the macrocycle between the *succ* and *ni* stations, the electrochemical behavior of model rotaxanes **5**−**8** (Chart 2) was investigated.

'Gate-closed' shuttle **7** incorporates a bulky silyl ether between the two stations which is large enough to preclude any shuttling yet should not prevent the formation of a variety of folded conformations; removal of this group to give **8** restores the possibility of redox-switched shuttling, thus generating a system closely analogous to **1**.

Compared to **1**, rotaxane **6** has a reduced length of alkyl spacer (C_2 in place of C_{12}), thus disallowing folded conformations involving multipoint interactions between the naphthalimide carbonyls and macrocycle amide protons.

In model compound **5**, methylation of the succinamide nitrogens prevents a folded conformation involving hydrogen bonding to these units (i.e., the *succ* unit in **5** can only act as a hydrogen-bond acceptor).

^{1}H NMR spectra of each of **5**−**8** in $CDCl_3$ show that the macrocycle sits over the *succ* station in each case, exactly as observed for **1**. The behavior of these model systems, together with other control experiments and observations, leads to a series of arguments showing that the observed CV effects in **1** are a result of the macrocycle shuttling along the thread.

(i) 'Gate-closed' rotaxane **7** (where shuttling is prohibited) shows a CV response (Figure 11a) identical to that of the thread **2** *not* rotaxane **1**, indicating that there is no hydrogen-bond

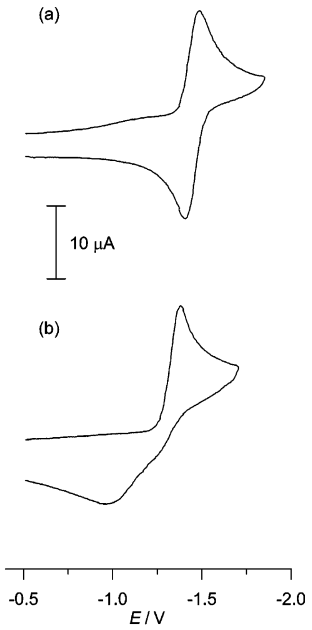

Figure 11. Cyclic voltammograms at 223 K of (a) **7** and (b) **8**. Experiments carried out on 0.5 mmol L^{-1} solutions in DMF with tetraethylammonium tetrafluoroborate (5×10^{-2} mol l^{-1}) as internal standard. Scan rate: 0.5 V s^{-1}. Working electrode: Pt.

stabilization of the naphthalimide radical anion as a result of folding in $\mathbf{7}^{-\bullet}$. However, the 'gate-opened' version **8** shows virtually identical CV behavior (Figure 11b) to rotaxane **1**, the only difference being that the dynamics are over a slightly longer time scale presumably as a result of the branching in the thread providing a small steric barrier to macrocycle translation.

(ii) Model rotaxane **6**, which is too short and rigid to allow multiple hydrogen bonds between the macrocycle and the *ni* station when the macrocycle is situated over the succinamide station, also shows very similar CV behavior to **1**, although over a much shorter time scale, reflecting the smaller amplitude of shuttling that is required.

(iii) Removing the possibility of hydrogen bonding to the amide protons of the *succ* station in **5** does not affect the CV response, suggesting that *all* the hydrogen bonds to the *ni*$^{-\bullet}$ station come from the macrocycle.

(iv) Molecular modeling studies show that folded conformations of $\mathbf{1}^{-\bullet}$ can only be stabilized by one or two hydrogen bonds from the macrocycle to the *ni* station due to geometrical constraints. Molecular dynamics simulations on such structures

indicate that the macrocycle would still shuttle along the thread in order to form multipoint hydrogen bonds to the naphthalimide unit.[29]

(v) The large anodic shift for reoxidation of the naphthalimide in $\mathbf{1}^{-\bullet}$ indicates extensive stabilization of the radical anion ($\Delta E^\circ = 0.51$ V; corresponding to $\Delta G = -11.8$ kcal mol^{-1}). This is equivalent to the formation of three or four strong hydrogen bonds which modeling shows can only arise in geometries where shuttling has occurred.[30]

(vi) If only one or two intramolecular hydrogen bonds were producing the shifts seen in the CV of **1**, a similar process could take place in the thread (**2**) using the succinamide amide protons as hydrogen-bond donors. This is clearly not the case as **2** exhibits an identical CV response to that of its *N*-methylated analogue (**9**).

(vii) For rotaxanes **1**, **5,** and **8** (dynamics in **6** are too fast to measure), more polar solvents accelerate the speed of the process, suggesting that breaking of hydrogen bonds is the rate-determining step, not formation of hydrogen bonds which one might expect in a folding mechanism.

(viii) It is known that alkyl chains fold several orders of magnitude faster than the dynamics observed in the current system.[31]

(ix) Folding a long alkyl chain is entropically unfavorable, and cyclic hydrogen-bonded conformations forming large rings of the type produced in the possible folded conformations of $\mathbf{1}^{-\bullet}$ are not often free energy minima.[32] In comparison, the entropy of activation calculated for shuttling in $\mathbf{1}^{-\bullet}$ ($\Delta S^\ddagger = 8.7 \pm 2$ cal K^{-1} mol^{-1}) is positive; the calculated enthalpy of activation ($\Delta H^\ddagger = 14.0 \pm 0.6$ kcal mol^{-1}) is also more consistent with a shuttling mechanism, where the rate-determining step is breaking of hydrogen bonds as opposed to forming bonds in a folding mechanism.

(x) The energy barrier determined for shuttling in the reduced state ($\Delta G_{298}^\ddagger = 11.4 \pm 1.2$ kcal mol^{-1}) is consistent with known energy barriers for shuttling between two degenerate stations in similar molecular shuttles[7a] and also with the energy barrier for pirouetting of the macrocycle in model rotaxane **3** (see above).

Given that folding cannot account for the multipoint hydrogen bonding that stabilizes the reduced naphthalimide in $\mathbf{1}^{-\bullet}$ nor can it account for the behavior of **8** mirroring that of **1** while that of **7** does not, the only process that satisfies the experimental behavior for these molecules is shuttling. We do not exclude the likelihood that folding occurs in some of these systems to some degree (e.g., *folded-ni*-$\mathbf{1}^{-\bullet}$, Figure 10). Indeed, there is evidence to support this in a few of the low-energy co-conformations identified in modeling studies (see above and ref 29). However, in all these low-energy co-conformations—folded or extended—the macrocycle has shuttled from the *succ* station to the $ni^{-\bullet}$ unit.

Conclusions

The use of electrochemical stimuli to manipulate intercomponent interactions provides a powerful method for both controlling and observing submolecular motion in hydrogen-bonded molecular shuttles. In the present benzylic amide macrocycle-based rotaxane system, the motion resulting from reduction and reoxidation of the naphthalimide station is unequivocally shown to be reversible shuttling of the macrocycle along the thread. This constitutes a molecular shuttle which exhibits remarkable positional integrity of the macrocycle on the thread in both oxidation states and rapid dynamics of the triggered shuttling between them. The simplicity of the structures involved and the process used to control the motion of the components augurs well for the development of molecular devices based on such systems.

Experimental Section

Synthesis. All synthetic procedures are reported in the Supporting Information.

Electrochemistry. Materials. All chemicals used were reagent grade. Tetrabutylammonium hexafluorophosphate (TBHF, Fluka) was used as supporting electrolyte as received. Tetrahydrofuran (LiChrosolv) was treated according to a procedure described elsewhere.[33] For the electrochemical experiments, the solvent was distilled into the electrochemical cell, prior to use, by a trap-to-trap procedure.

Instrumentation and Measurements. The one-compartment electrochemical cell was of airtight design, with high-vacuum glass stopcocks fitted with either Teflon or Kalrez (DuPont) O-rings to prevent contamination by grease. The connections to the high-vacuum line and to the Schlenck containing the solvent were made by spherical joints fitted with Kalrez O-rings. The pressure measured in the electrochemical cell prior to performing the trap-to-trap distillation of the solvent was typically 1.0 to 2.0×10^{-5} mbar. The working electrode consisted either of a 0.6 mm diameter platinum wire (0.15 cm^2 approximately) sealed in glass or platinum disk ultramicroelectrodes (with radii from 5 to 62.5 μm) also sealed in glass. The counter electrode consisted of a platinum spiral, and the quasi-reference electrode was a silver spiral. The quasi-reference electrode drift was negligible for the time required by a single experiment. Both the counter and reference electrodes were separated from the working electrode by ~0.5 cm. Potentials were measured with the ferrocene or decamethylferrocene standards and are always referred to saturated calomel electrode (SCE). $E_{1/2}$ values correspond to $(E_c + E_a)/2$ from CV. Ferrocene (decamethylferrocene) was also used as an internal standard for checking the electrochemical reversibility of a redox couple. The temperature dependence of the relevant internal standard redox couple potential was measured with respect to SCE by a nonisothermal arrangement.[34] Voltammograms were recorded with an AMEL Model 552 potentiostat or a custom-made fast potentiostat controlled by either an AMEL Model 568 function generator or an ELCHEMA Model FG-206F. Data acquisition was performed by a Nicolet Model 3091 digital oscilloscope interfaced to a PC. Temperature control was accomplished within 0.1 °C with a Lauda thermostat. The minimization of ohmic drop was achieved through the positive feedback circuit implemented in the potentiostat. Digital simulation of cyclic voltammetric experiments: The CV simulations were carried out by the DigiSim 3.0 software by Bioanalytical Systems Inc. All the fitting parameters (see Supporting Information) were chosen so as to obtain a visual best fit over a 10^{2-}-10^3-fold range of scan rates.

Acknowledgment. We thank Andrea Altieri for the preparation of model rotaxane **4**. This work was supported through the EU TMR Network contract FMRX-CT96-0059, the EPSRC, the University of Bologna ("Funds for Selected Research

(29) Indeed, recent molecular modelling studies by other groups reinforce this view: Zheng, X.; Sohlberg, K. *J. Phys. Chem. A* **2003**, *107*, 1207−1215.
(30) In complexes with 2,6-diamidopyridines, three hydrogen bonds to a *ni* unit cause a stabilization of ~0.2 V: see refs 14b and 14c.
(31) Zachariasse, K. A.; Maçanita, A. L.; Künhle, W. *J. Phys. Chem. B* **1999** *103*, 9356−9365.
(32) Gellman, S. H.; Dado, G. P.; Liang, G.-B.; Adams, B. R. *J. Am. Chem. Soc.* **1991**, *113*, 1164−1173.
(33) Carano, M.; Ceroni, P.; Mottier, L.; Paolucci, F.; Roffia, S. *J. Electrochem. Soc.* **1999**, *146*, 3357−3360.
(34) Yee, E. L.; Cave, R. J.; Guyer, K. L.; Tyma, P. D.; Weaver, M. J. *J. Am. Chem. Soc.* **1979**, *101*, 1131−1137.

Topics"), MIUR (PRIN 2002, prot. 2002035735), and CNR (Agenzia 2000). F.G.G. and D.A.L. are Marie Curie (FMBI-CT97-2834) and EPSRC Advanced (AF/982324) Research Fellows.

Supporting Information Available: Full synthetic procedures, crystallographic information, fitting parameters for the simulation of cyclic voltammetry curves, additional cyclic voltammograms illustrating the effect of scan rate and of temperature on the electrochemical response of compounds **1**, **2**, **6**, **7**, and **8**, procedure for spin polarization transfer by selective inversion recovery (SPT-SIR) experiments, and Eyring plot for the variation of shuttling rates with temperature (PDF and CIF). This material is available free of charge via the Internet at http://pubs.acs.org.

JA0352552